The Diagnosis of Multifaults in Analogue Circuits Using Multilayer Perceptrons

Y. Maidon[1], B. W. Jervis[2], N. Dutton[2], and S. Lesage[1]

1 Laboratoire IXL, Université Bordeaux I, 352 cours de la Libération, 3305 TALENCE, France
2 School of Engineering, Sheffield Hallam University, Pond Street, Sheffield, S1 1WB, England.

Abstract. *It is shown, by means of an example, how multiple faults in bipolar analogue integrated circuits can be diagnosed, and their resistances determined, from the magnitudes of the Fourier harmonics in the spectrum of the circuit responses to a sinusoidal input test signal using a two-stage multilayer perceptron (MLP) artificial neural network arrangement to classify the responses to the corresponding fault. A sensitivity analysis is performed to identify those harmonic amplitudes which are most sensitive to the faults, and also to which faults the functioning of the CUT is most sensitive. The experimental and simulation procedures are described. The procedures adopted for data pre-processing and for training the MLPs are given. One hundred percent diagnostic accuracy was achieved, and most resistances were determined with tolerable accuracy.*

I. Introduction

Various methods [1- 4] have been developed for analogue circuit testing. However, they typically require too many test points and need extensive complicated computation. For these reasons they have not gained widespread acceptance in production. The increased size and complexity of modern circuits has meant that the "bed of nails" test technique has become impractical because too many external test points are needed. This has led to the introduction of alternative built-in self-test (BIST) structures for analogue circuits [5, 6, 7].

A more recent approach has been to apply the pattern recognition capabilities of artificial neural networks (ANNs) to diagnose faults by associating patterns in the test response data with the corresponding faults. Rutkowski [8] used a neural network to achieve the diagnosis by recognising patterns in the measured nodal voltages. Meador et al. [9] showed that feedforward neural networks provided a cost efficient method for the diagnosis of open and short circuit (hard) faults in IC operational amplifiers in a production environment. The network was used to recognise patterns in the time and frequency domain responses of fault-free and defective circuits. It offered an order of magnitude improvement in diagnostic speed while consistently performing as well as or better than other classifiers in terms of accuracy. The method reported here uses fewer test points than in [8] and in contrast to [9] is extended to soft faults. Spina and Upadhyaya [10] performed signature analysis using ANNs to recognise the fault-free and faulty responses of a common emitter amplifier to input white noise. A classification ambiguity for two of the faults remained unresolved. Ambiguities are resolved in the work reported here.

Supply current monitoring has been investigated in simulations for testing analogue and mixed signal circuits [11, 12]. In both cases the tests were go/no go tests of single faults. One hundred percent diagnosis of a single gate oxide short (GOS) fault in a MOSFET transistor of an operational amplifier has been achieved in simulation by associating the patterns of the supply current responses to test signals at the input with the simulated fault using artificial

neural networks [13, 14]. It was further shown [14] that with varying degrees of accuracy it was possible to estimate the resistance of the short circuit and its location between the source and drain.

In another method the faults in a circuit have been diagnosed from the signature of the spectrum of its response to a sinusoidal input signal [15, 16].

In this paper a combination of the above method of using an ANN to diagnose GOS faults from the signature of the supply current response of the circuit with the method of signature analysis of the response spectrum is described for the diagnosis of multiple faults in an analogue bipolar transistor circuit. The diagnosis was based upon the signature formed from selected harmonic components of the spectrum of the output response of the circuit to an input stimulus. This has been achieved both in simulations and experimentally. Diagnosis was performed in the frequency domain because of the ready availability of spectrum analysers for circuit testing.

Faults in resistors, capacitors, diodes, and transistors are usual in bipolar circuits [12] and so the diagnosis of this type of fault was investigated in this work. Typically, the base-emitter, collector-emitter, and base-collector resistances are modified. Electrical overstress and electrostatic effects can reduce the resistances, while bulk and interface failure mechanisms can either increase or decrease them [12].

II. Approach

Multilayer perceptron (MLP) artificial neural networks (ANNs) [17] were used in this work because their outputs may represent the class associated with an input data vector and are also quantitatively mappable to associated parameter values. In the present context the input vector consists of the magnitudes of the Fourier harmonics of the response waveforms owing to the input stimulus, and the class represents the type of circuit fault, while the outputs map to the resistance values of the faults. The networks were trained using the back-propagation (BP) algorithm [18]. The largest MLP contained 21 nodes, and required a total of 123 weight and threshold values. For each fault 1239 values of resistance were used in the simulations for network training and a further 958 for testing. These were sufficient to ensure that the MLPs generalised and were not overtrained to a particular type of input vector.

The circuit under test (CUT) was a differential amplifier (Figure 1) with current mirror, included in an ASIC (BiCMOS Semicustom Array from Integrated Associates Incorporated company), and was chosen as a simple example for testing the feasibility of the developed methods [15, 16].

A sinusoidal signal was applied to the input of the circuit under test and the spectral response of the entire circuit was measured when the circuit was in a steady state. Because of the symmetrical properties of the circuit, the spectral response of the circuit without faults nearly always contained odd harmonics.

To illustrate this method, the intrinsic resistance values re and rb in the Hspice model were varied. In effect, these intrinsic resistances can be increased by adding an external resistor (r_{B2},

r_{E1} and r_{E2}, Figure 1). The type of simulated fault corresponds to the technological problems of dopage of the extrinsic zones or an open contact problem before metallisation.

The sensitivity of fault diagnosis by harmonic analysis was proved by computing the sensitivity factors:

$$S_{i,j} = \frac{\Delta H_i}{H_i} \Big/ \frac{\Delta x_j}{x_j}$$

where S is the Sensitivity Factor, H_i = amplitude of the i^{th} harmonic, and x_j = value of the j^{th} parameter.
The influence of the beta1 parameter on the magnitude of the Sensitivity Factor S is shown in Figure 2 for a one fault circuit. It shows that this factor is largest for the even harmonics, but even these have a very low magnitude for this type of circuit.

It was verified by simulation with good precision that the values obtained by modifying the parameters re and rb of the Hspice transistor model and the values obtained by modification of the external resistances (r_{B2}, r_{E1} and r_{E2}) added to the nominal Hspice model were similar. The similarity between the practical measurements and Hspice simulations was also verified.

For the construction of the fault dictionary, the CUT was simulated using Hspice software. The chosen resistances which represented faults were varied. The value of the DC component, the amplitudes of the harmonics H_1 to H_3 (taken from the file *.lis), and the corresponding values of the faults (here r_{B2}, r_{E1} and r_{E2}) were recorded. The maximum and minimum values of the faults were carefully chosen. In effect the fault dictionary technique implies that only the faults within this range can be detected. The detection of catastrophic faults like short and open circuits is not possible if they are not present in the dictionary (as in this case).
The simulated raw data was obtained from the *.lis file created by the Hspice software. The measurements were made using the test setup shown in Figure 3 which automatically records the values of the different harmonics and the DC values.

III. Data Pre-processing

The training data vectors were assessed as to their suitability for the training of the MLPs. The data vector elements were the magnitudes of the DC term and of the first three harmonics of the FFT of the output voltage response waveform. The magnitudes of harmonics 2 and 4 were considerably smaller than those of the DC component and of the first harmonic, as seen in Figure 4a . In order to reduce the disparities in the values of the training and test vector elements and of the weights, and for the purpose of visual inspection, the values of harmonics 2 and 3 were multiplied by 10, Figure 4b . Subsequently for the purpose of training the MLPs the resulting harmonic magnitudes were scaled so that all values lay between 0 and 1.0. The latter was achieved by normalising all values to the highest. By reducing the disparities, the MLP was more rapidly trainable.

The plots of harmonic magnitude versus harmonic number, including the DC term, with fault resistance as parameter, were inspected next for each fault. See Figures 5a, 5b, and 5c respectively. Note that in the figures the solid line represents the fault-free case. The presence of faults r_{B2}, r_{E1} and r_{E2} were indicated in a binary format such that, for example, (101)

indicated (r_{B2} faulty, r_{E1} fault-free, r_{E2} faulty). The plots of magnitude versus harmonic number for fault type (001) subdivided into two characteristic sets of curves, $(001)_a$ and $(001)_b$ respectively. These plots are shown in Figures 5a, 6a, and 6b respectively). Similarly, the (010) and the (100) faults subdivided into $(010)_a$, $(010)_b$ and $(100)_a$, $(100)_b$ characteristic curves. Of these, the $(100)_b$, $(010)_b$ and $(100)_b$ curves were very similar, suggesting that it might be difficult to distinguish between the different types of fault using MLPs, ie classification ambiguities might occur.

The following strategy was adopted to minimise the number of ambiguous classifications of fault-type. If the outputs (i, j, k) of the MLP were approximately zeros or ones then the classification was unambiguous. However, if the output values i, j, k were intermediate between approximately 0 and approximately 1, then the classification was considered ambiguous. To overcome this a program called "TABLE" was written. For each output the threshold value above which the output could be considered a 1, and below which it was to be considered a 0 was adjustable. Having first trained the MLP, test vectors were applied and the thresholds set in TABLE varied. The program then set the outputs to 1 or 0 according to the threshold value. A table of the number of ambiguous decisions for the test data at each threshold level was then produced by TABLE. The threshold values which minimised the number of ambiguities were thus determined. These threshold values were then used in a second program called ROUND, which simply converted all the test outputs of the MLP to ones or zeros to indicate the class, ie the fault type.

Another program, SHUFFLE, was written and used to randomise the order of presentation of the training data to the MLP in order to avoid biasing of the network parameters which can occur when the data is presented in the same order at each iteration of the training data set.

IV. Experimental measurement procedure

Measurements were made using an experimental setup composed of a function generator (HP3325A), a spectrum analyser (HP3588A), a DC multimeter (HP3458A), and the circuit under test, all of them managed by a PC via the IEEE488 Data Bus (Figure 3). The PC was linked to a Sun workstation by an Ethernet network to allow bidirectional transfer of information between the PC and the Sun. The function generator was programmed to deliver the same signal as used in the Hspice simulations. The spectrum analyser and multimeter sent the DC values and the harmonic amplitudes to the computer for storage in a results file. The PC was used to take the measurements. The Sun workstation was used to perform the Hspice simulation, build the dictionary, and to train and validate the MLPs using SNNS (Stuttgart Neural Network Simulator). Then the PC was used to make a statistical analysis of the values of the resistances given by the MLPs.

The values of the fault choice for r_{B2} were [1Ω, 1kΩ, 2.2kΩ, 3.3kΩ and 5.6kΩ] and for r_{E1} or r_{E2}, they were [1Ω, 27Ω, 82Ω, 150Ω and 330Ω]. For these 3 resistors 5 values per fault were used. Thus, $5^3 = 125$ measurements were made to an accuracy of 1mV. The circuit was designed for easy access to the resistors r_{B2}, r_{E1} and r_{E2}, thus allowing rapid manual modification.

Thermal errors were avoided by placing the CUT in a thermally stable environment. For example, a variation in temperature of 1°C causes a change of 0.5mV in the DC value and of

10mV in the first harmonic. Therefore all measurements were taken at a fixed temperature of 25°C.

V. Simulation procedure

The data was obtained from the Hspice software simulations. The CUT was stimulated by a sinusoidal signal of 50mV, at 1kHz. The simulations were performed for the same temperature as the measurement chamber temperature (.temp 25). The data simulated or measured was normalised before being transferred and used in the MLPs.

Catastrophic faults like short circuits or open circuits were not investigated. The resistors r_{E1} and r_{E2}, were varied from 0Ω, corresponding to a fault free circuit for which the intrinsic resistance values are equal to the nominal Hspice model, to 380Ω. Resistor r_{B2} was varied from 0Ω to 10kΩ. Thirteen values per fault were chosen, giving a dictionary containing 2197 patterns {(number of values)$^{(\text{number of faults})}$ = 13^3}. The intermediate values were spaced approximately linearly between the two extremes (depending upon the values of the standard resistors).

The similarity between the values obtained by measurement and the values obtained by simulation was verified.

VI. MLP procedures

It was necessary to both train the MLPs and to optimise their architectures in order to effect the diagnosis. There were four inputs to the MLPs which corresponded to the dc and first three harmonic magnitudes of the FFT components of the spectrum of the output voltage. In each case there was only one output (see below). The optimisation was achieved for each network used by experimenting with different numbers of nodes in the two hidden layers. The architectures which resulted in acceptably small training errors, the clearest indications of fault-type (given by the values of the output nodes), and the least number of nodes were adopted. Some of the MLPs were subsequently reduced in size by eliminating those nodes which made disproportionately small contributions to the output. These were identifiable since the commercial MLP program used gave an indication of the relative use of the nodes. The training of the network was also assessed in terms of accuracy of classification of the test data. Further training or modifications were undertaken if the testing accuracy was inadequate. Sigmoidal transfer functions were implemented for the hidden layers and output nodes.

Considerable effort was spent in determing an MLP arrangement which would allow the diagnosis of both the type and the resistance of multiple faults in the circuit. The solution was to use a primary layer of three MLPs, each trained to detect one of the three fault types investigated, with a secondary layer of three MLPs to indicate the values of the resistances of the corresponding detected faults. In this way the presence of any combination of one, two, or three faults could be detected and their resistance values obtained. The inputs to the MLPs were the pre-processed magnitudes of the components of the spectrum as described above. This system is shown in Figure 7.

An input vector was first created for the fault-free case in which the resistances had their nominal values of rb_2 = 14 Ω, re_1 = 0.3mΩ, and re_2 = 0.1mΩ. Then a training vector set of 1239 examples and a test vector set of 958 examples was created for each fault type by

generating further examples by systematically increasing the resistances of first each fault in turn, and then repeating for multiple faults. In this way all possible combinations of one, two, or three faults were simulated. The range of resistors was from 0 to 10kΩ for r_{B2} (corresponding to a variation of rb_2 from its nominal value (14Ω) to 10kΩ), from 0 to 380Ω for r_{E1} and r_{E2} (corresponding respectively to a variation of re_1 and re_2 from the nominal value to 380Ω). The three fault-detection networks were trained as described above to detect whether a fault had occurred, while the three fault valuation networks were trained to give an output which represented the resistances of the indicated faults. In the test mode the faults present were thus indicated and their resistance values given.

VII. Evaluation procedure

In order to evaluate the accuracy achieved by the fault valuation networks, the MLP output data were loaded into a spreadsheet package, then converted to ohms by multiplying by the appropriate factor. The differences between the predicted resistances and the known values were calculated. For each fault type these differences were grouped according to the size of the errors, and the percentage of faults within a number of different error ranges was determined, see Table 1.

VIII. Results

One hundred per cent diagnostic accuracy was achieved for identifying the fault type using the test data. Some no-fault examples were missed by the fault-detection MLP, but were identified by the low resistance values at the fault valuation MLP. Table 1 shows the errors obtained in determining the values of the different fault resistances. From this table it is seen that over 50% of the fault resistance values were found to be within 1Ω of the known value. In the case of the (001), or rb_2 fault, 30.6% of the values are in error by >1kΩ. This seems a disappointingly bad result. However, this was found to correspond to the error in the largest resistance values, and therefore only represented a smaller percentage resistance error. This finding was generally true, ie the largest errors occurred for the larger resistances and represented relatively small percentage errors. Furthermore the results for each fault reflect the different amounts of training to which each fault valuation network was subjected.

IX. Discussion

It has been demonstrated by experiment and simulation that the magnitudes of harmonics 0 to 3 of the Fourier spectrum of the response of the analogue CUT to a sinusoidal test input signal may be used both to diagnose and also to quantify the possible three multiple faults with the highest sensitivities which can occur. This was achieved using a two-stage MLP arrangement, in which each of the three MLPs in the primary layer were used to detect the presence of the fault-type upon which it was trained, and the three MLPs in the secondary layer yielded the corresponding values of the fault resistance. Since the MLP output error is known for each resistance value used for each fault, it is possible to convert the MLP output values to the precise resistance values. This will yield 100% resistance value accuracy. This method is thought to be extendable to the diagnosis of multiple faults in other circuits. Besides serving as a test for faults, the method will be useful in quality control, since the faults are both diagnosed and quantified. This will assist the production engineer to identify production process errors. In order to achieve good experimental results care has to be taken to both stabilise the temperature of the CUT and of the active probe and to ensure the measurement

equipment is calibrated. The method is appropriate when a spectrum analyser is available as part of the test equipment. This may not always be the case, and so in future work the application of the method in the time domain to the output voltage and with alternative test signals will be investigated. It is possible that a simpler MLP structure could be found to effect the diagnosis and quantification of faults in the time domain. This is because there may be more useful information available in the voltage waveform than there is in the magnitude spectrum.

X. Conclusions

Multiple faults in bipolar analogue integrated circuits can be diagnosed, and their resistances determined, from the magnitudes of the Fourier harmonics in the spectrum of the circuit responses to a sinusoidal input test signal using a two-stage multilayer perceptron artificial neural network arrangement to classify the responses to the corresponding fault. This technique has applications to the process control of such circuits, as well as for test.

XI. References

[1] J. W. Bandler and A. E. Salama, "Fault diagnosis of analog circuits.", Proc. IEEE, vol. 73, no. 8, Aug. 1985.

[2] G. N. Stenbakken and T. Souders, "Test-point selection and testability measures via QR factorization of linear models.", IEEE Trans on Instrumentation and Measurement, vol. IM-36, No. 2, June, 1987.

[3] G. N. Stenbakken and T. Souders, "Ambiguity groups and testability.", IEEE Trans on Instrumentation and Measurement, vol. 38, No. 5, Oct. 1989.

[4] H. Dai and T. Souders, "Time domain testing strategies and fault diagnosis for analog systems.", IEEE Trans on Instrumentation and Measurement, vol. 39, No. 1, Feb. 1990.

[5] C. Wey and S. Krishan "Built-in self-test (BIST) structures for analog circuit fault diagnosis with current test data.", IEEE Trans on Instrumentation and Measurement., vol. 41, no. 4, Aug., 1992.

[6] A.A. Hatzopoulos, S. Siskos, and J. Kontoleon, "A complete scheme of built-in self-test BIST structure for fault diagnosis in analogue circuits and systems", IEEE Trans Instrumentation and Measurement, vol 42, pp 689-694, June, 1993

[7] G. Russell and D. Learmouth, "Testing analogue functions using M-sequence", Electronics Letters, vol 29, No 21, pp 1818-1819, 14 Oct. 1993.

[8] G. Rutkowski "A Neural approach to fault location in nonlinear DC circuits", Proc. Int. Artificial Neural Networks Conf, Brighton, 1992, pp. 1123-26.[9] J. Meador, A. Wu, C. T. Tseng and T. S. Lin, "Fast diagnosis of integrated circuit faults using feedforward neural networks.". Int Joint Conf. on Neural Networks. IJCNN 91 Seattle. vol. 1. pp 269-273.

[9] J. Meador, A. Wu, C. T. Tseng and T. S. Lin, "Fast diagnosis of integrated circuit faults using feedforward neural networks", Int. Joint Conf. on Neural Networks, IJCNN 91 Seattle, vol. 1, pp 269-273.

[10] R. Spina and S. Upadhyaya, "Fault diagnosis of analog circuits using artificial neural networks as signature analyzers", Procs. 5th Ann. IEEE Int. ASIC Conf. Exhib., 1992, pp 355-358.

[11] I.M. Bell, D.A. Camplin, G.E. Taylor and B.R. Bannister, "Supply current testing of mixed analogue and digital ICs", Electronics Letters, vol 27, No 17, pp 1581-1583, 18 Aug. 1991.

[12] D. K. Papakostos and A. A. Hatzopoulos, "Supply current testing in linear bipolar ICs", Electronics Letters, vol. 30, No. 2, pp 128-130, 20 January, 1994.

[13] S. Yu, B. W. Jervis, K. R. Eckersall, I. M. Bell, A. G. Hall, and G. E. Taylor, "Neural network approach to fault diagnosis in CMOS opamps with gate oxide short faults", Electronics Letters, vol. 30, No. 9, pp 695-696, 1994.

[14] P. Collins, S. Yu, K. R. Eckersall, B. W. Jervis, I. M. Bell, and G. E. Taylor, "Application of Kohonen and supervised forced organisation maps to fault diagnosis in CMOS opamps", Electronics Letters, vol. 30, No. 22, pp 1846-1847, 27 October, 1994.

[15] Y. Maidon, S. Lesage, P. Fouillat, C. Bouvet, J.P. Dom, "FFT analysis for fault diagnosis on analogue integrated circuits : a new approach", 6th European Symposium on Reliability of Electron devices, Failure physics and analysis, Arcachon - France, 3-6 October 1995.

[16] Y. Maidon, S. Lesage, P. Fouillat, Y. Deval, J.P. Dom, "Analogue Circuit Testing for Fault Diagnosis by FFT Analysis", International Mixed Signal Testing Workshop, Grenoble - France, 20-22 June 1995.

[17] Lippman, R.P., "An introduction to computing with Neural Nets", IEEE ASSP Magazine, pp 4-22, April 1987.

[18] D. E. Rumelhart, G. E. Hinton, and R. J. Williams, "Learning representations by back-propagating errors", Nature, No 132, pp 533-536, 1986

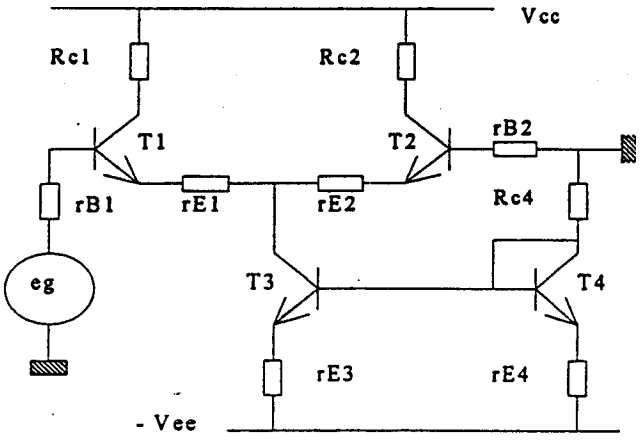

Figure 1.

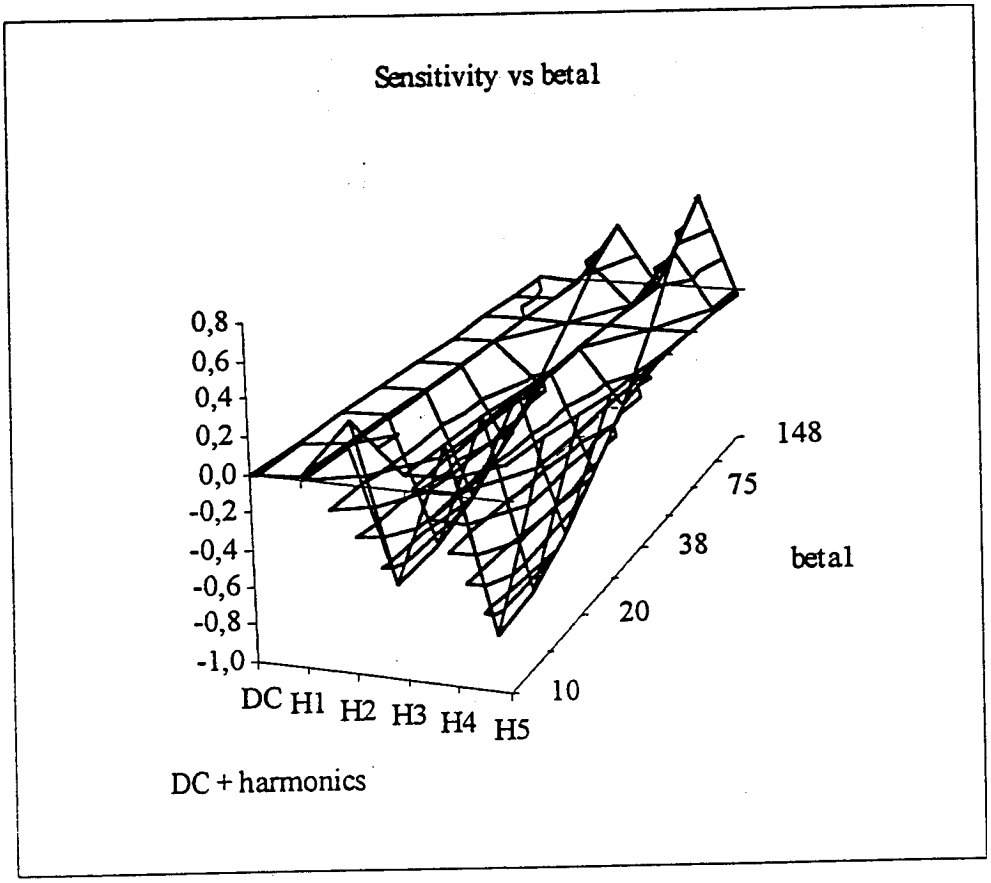

Figure 2.

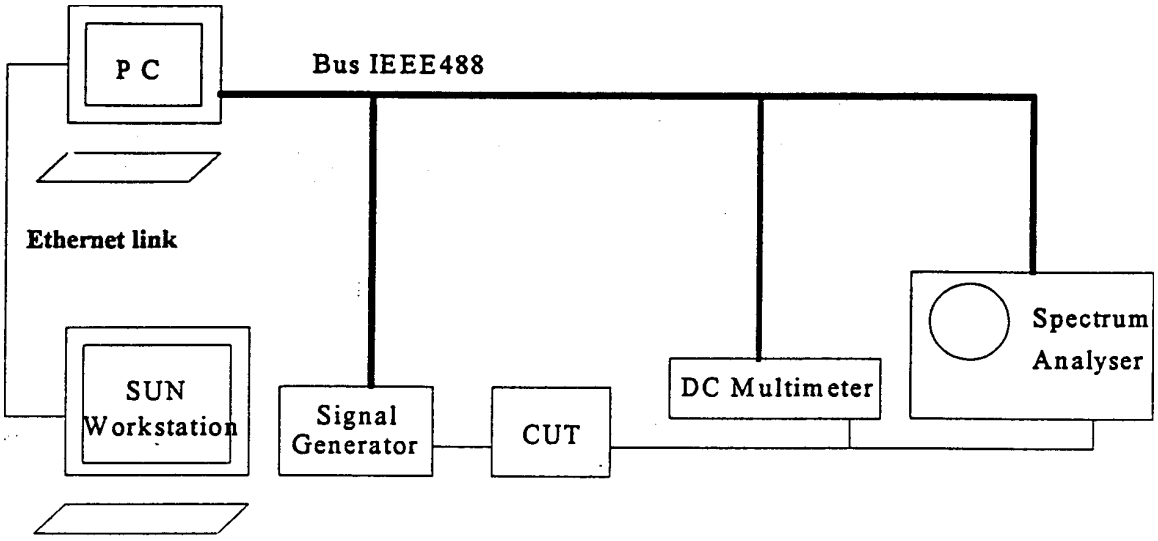
P C
Bus IEEE488
Ethernet link
SUN
Workstation
Signal
Generator
CUT
DC Multimeter
Spectrum
Analyser

Figure 3.

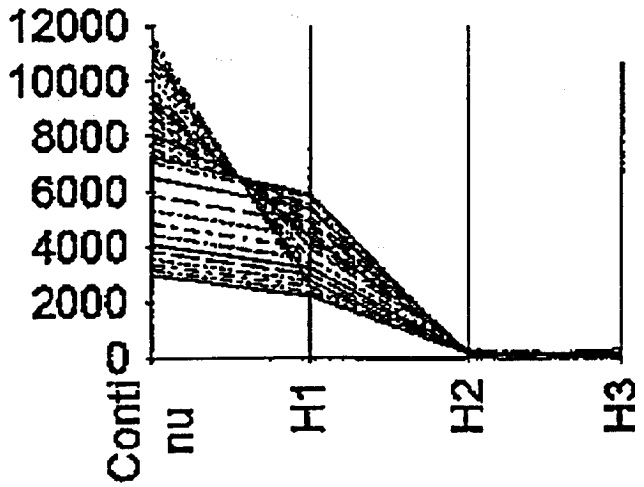

Figure 4a

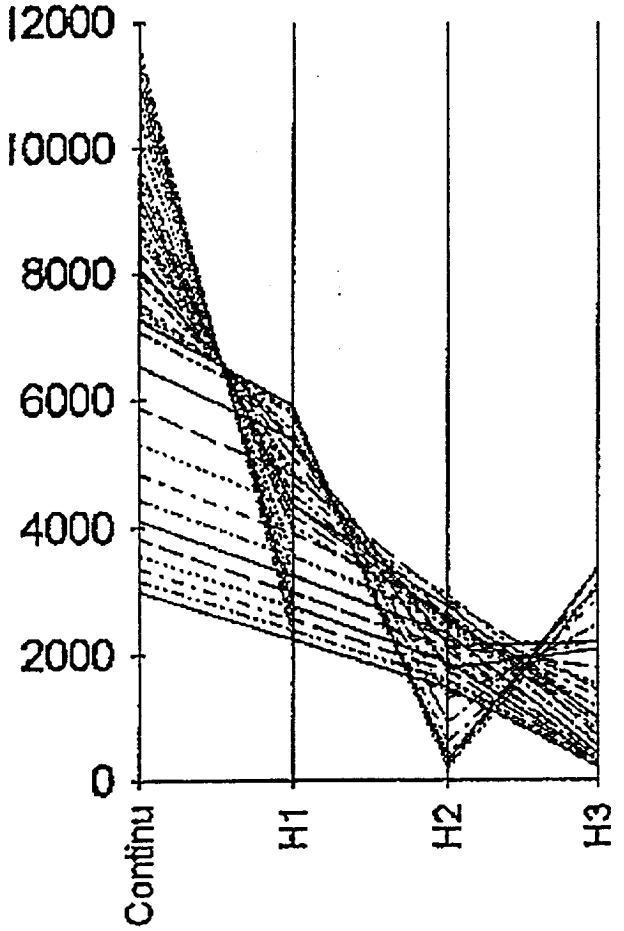

Figure 4b

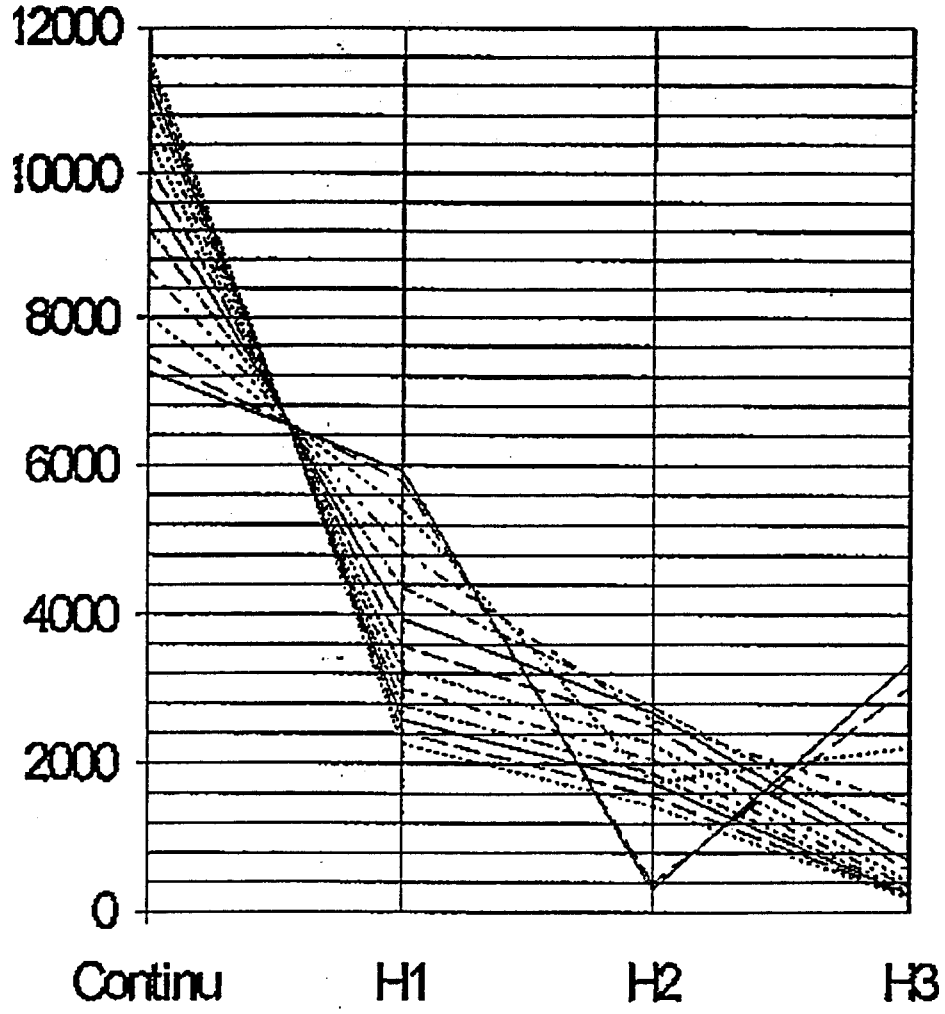

Figure 5a

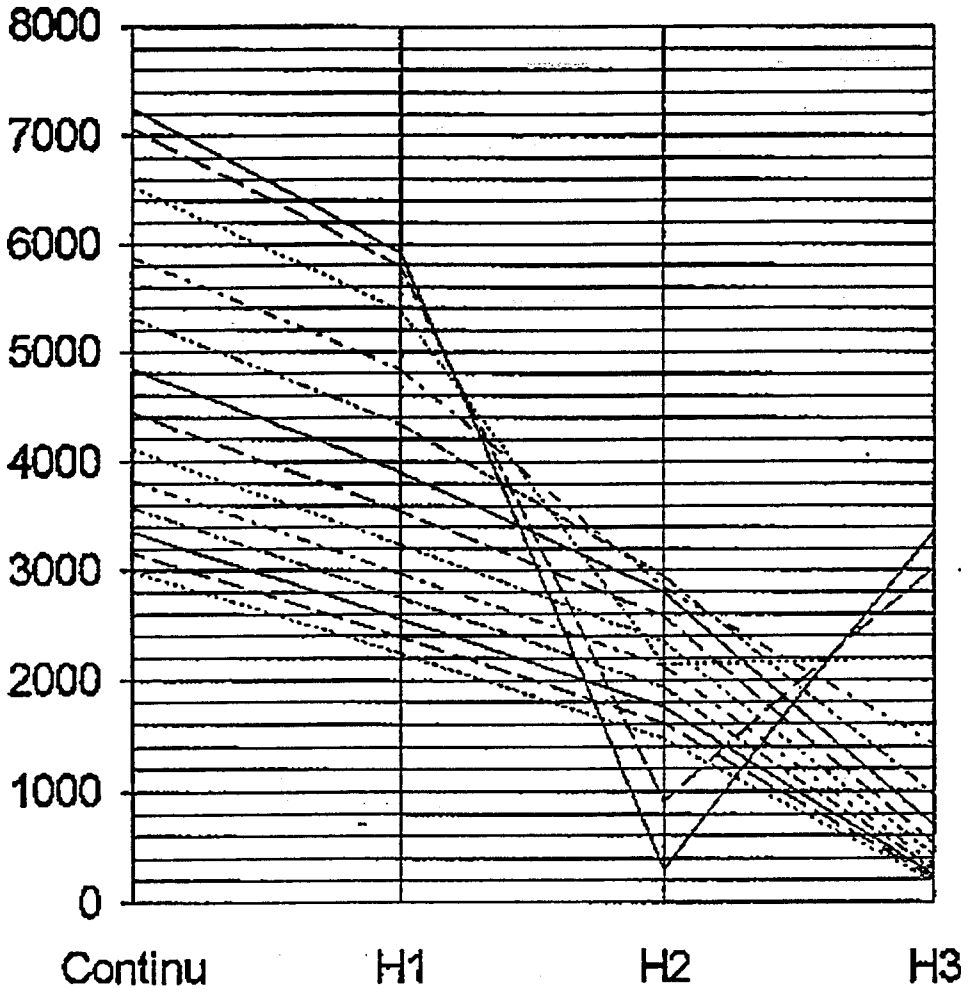

Figure 5b

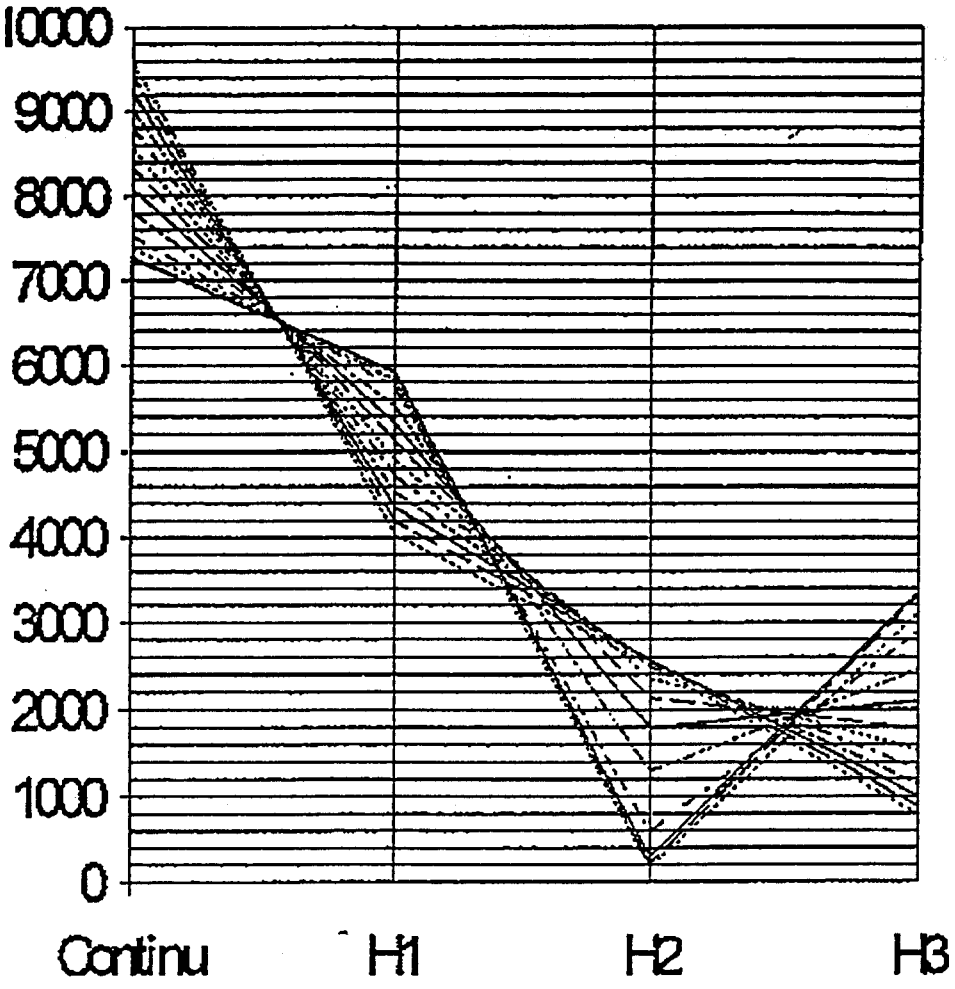
10000
9000
8000
7000
6000
5000
4000
3000
2000
1000
0
Continu
H1
H2
H3

Figure 5c

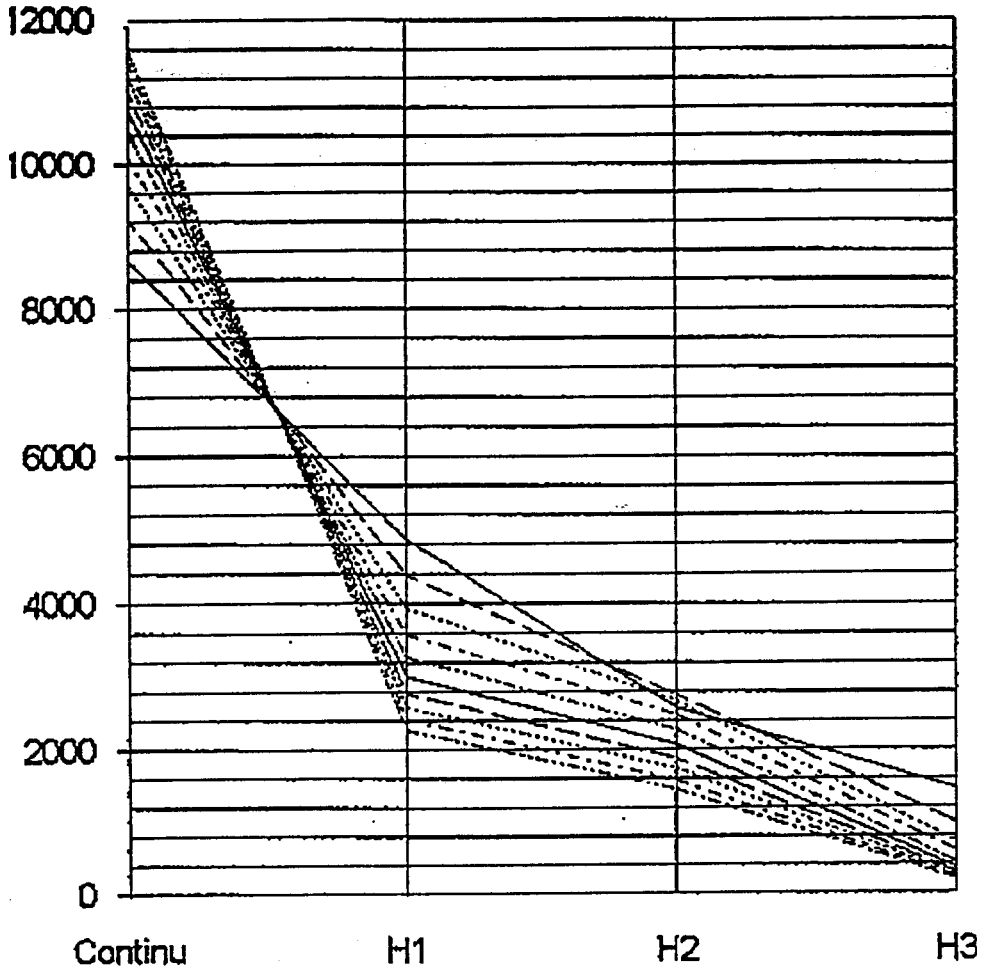

Figure 6a

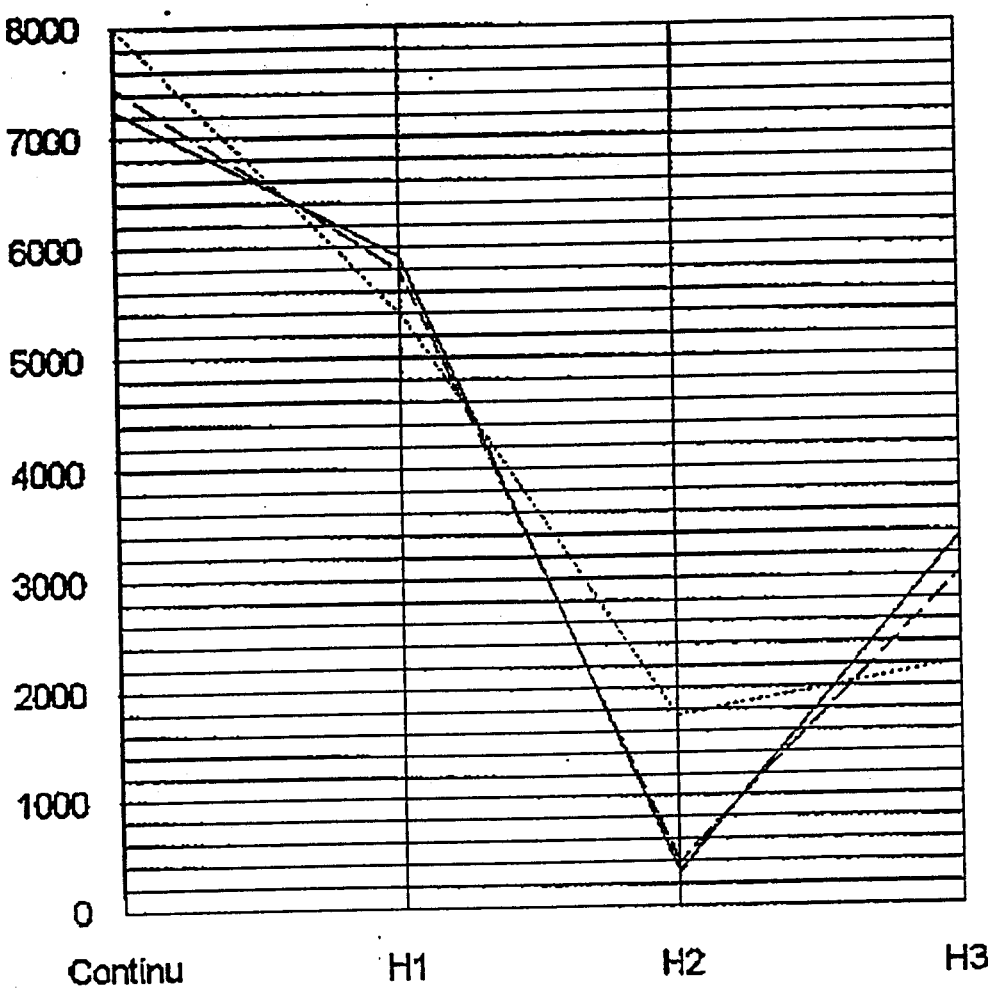

Figure 6b

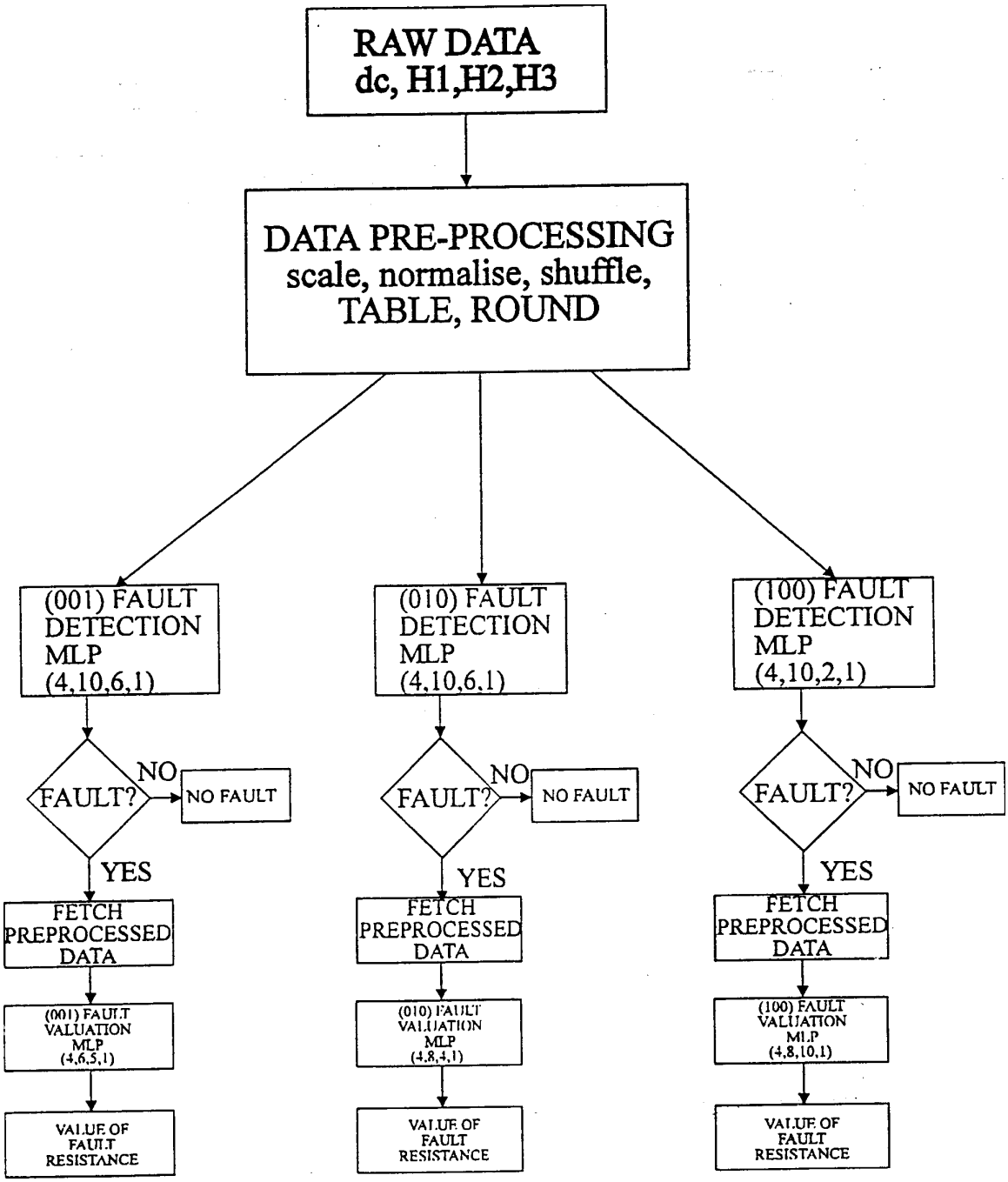

Figure 7

napixl8

Figure Captions

Figure 1 : Circuit Under Test.
Figure 2 : Sensitivity vs. Beta1.
Figure 3 : Experimental Test Setup.
Figure 4a : Harmonic magnitudes of the fault-free circuit
Figure 4b : Harmonic magnitudes after treatment.
Figure 5a : Harmonic magnitudes relating the fault r_{B2}.
Figure 5b : Harmonic magnitudes relating the fault r_{E1}.
Figure 5c : Harmonic magnitudes relating the fault r_{E2}.
Figure 6a : First part of the figure 5a.
Figure 6b : Second part of the figure 5a.
Figure 7 : Organisation of the MLPs.

Table 1. Errors in determining the fault resistance values.

Based on 1239 training vectors per fault type.

Fault type	Resistance range (Ω)	Error range (Ω)	% Faults
(001), rb_2	0-10k	±1	53.3
		2-10	0
		10-100	1.3
		100-500	4.8
		500-1k	9.9
		>1k	30.6
(010), re_1	0-280	±1	78.2
		2-5	5.08
		5-10	3.31
		10-20	3.31
		20-30	6.78
		>30	3.31
(100), re_2	0-280	±1	65.7
		2-5	5.81
		5-10	10.65
		10-20	10.0
		20-30	4.12
		>30	3.71